

Supporting Information For

Extremely supercharged proteins in mass spectrometry: Profiling the acidity of electrospray generated droplets, narrowing charge state distributions, and increasing ion fragmentation

Muhammad A. Zenaidee and William A. Donald

School of Chemistry, University of New South Wales, Sydney, New South Wales, 2052 Australia

Table of Contents

Title page	1
Table of Contents	2
Table S1. Average charge states of cytochrome <i>c</i> formed by use of different spray voltages	3
Table S2. Dipole moment and surface tension values of superchargers	4
Table S3. Effects of acid concentration on the CSDs of protonated cytochrome <i>c</i>	5
Table S4. ESI source conditions for electrosprayed protein ions	6
Table S5. Acid volatility data	7
Figure S1. Average charge states of protonated cytochrome <i>c</i> ions and extent of acid adduction plotted as a function of gas phase basicity and proton affinity values	8
Figure S2. Average charge states of protonated cytochrome <i>c</i> ions vs. acid volatility data	9
Figure S3. Average charge states of protonated cytochrome <i>c</i> ions plotted for each anion in order of the Hofmeister series	10
Figure S4. Effects of acids on the ESI mass spectra of protein/peptide ions without SCs	11
Figure S5. Widths of protein ion CSDs vs. acid pK_a for different proteins	12
Figure S6. Widths of protonated cyt <i>c</i> ion CSDs vs. acid pK_a for different superchargers	13
Figure S7. Effects of solvent on the ESI mass spectra of protonated cyt <i>c</i> ions	14
Figure S8. Effects of solvent on the average charge states of cyt <i>c</i> ions without SCs and with high concentrations of organic solvents	15
Figure S9. ESI and ECD mass spectra for protonated ubiquitin	16
Figure S10. Relative ECD-MS fragment ion abundances for [ubiquitin, 13H] ¹³⁺ and [ubiquitin, 17H] ¹⁷⁺	17
Details of experiments, data analysis, and materials	18
Discussion of Hofmeister anions	21
References	21

Table S1. Average charge states obtained by ESI of aqueous solutions containing 5 μ M cytochrome *c*, 0.5% (v/v) acetic acid, and 5% 4-vinyl-1,3-dioxalan-2-one as a function of the temperature ($^{\circ}$ C) of the capillary entrance to the MS for different potential values applied to the capillary entrance (V_c) and tube lens (V_t) of the ESI-MS source.

<i>T</i>	($V_c = 45$; $V_t = 9$)	($V_c = 60$; $V_t = 11$)	($V_c = 85$; $V_t = 35$)
250 $^{\circ}$ C	21.0 \pm 0.1	21.8 \pm 0.1	21.6 \pm 0.2
300 $^{\circ}$ C	21.8 \pm 0.2	21.7 \pm 0.2	21.7 \pm 0.1
350 $^{\circ}$ C	22.0 \pm 0.1	21.7 \pm 0.1	21.9 \pm 0.1
400 $^{\circ}$ C	22.1 \pm 0.1	22.2 \pm 0.1	22.6 \pm 0.2
450 $^{\circ}$ C	22.7 \pm 0.2	22.6 \pm 0.2	22.7 \pm 0.1

Table S2. Dipole moment and surface tension values of superchargers (SC). The standard deviation of three replicate measurements were < 1 mN/m units

SC ^a	μ (D) ^b	γ (mN/m) ^b Previous work	γ (mN/m) This work
BC	5.1 ^c	-	36
4V	5.6 ^c	-	40
PC	5.4 ^d	41.1 ^e	41
EC	4.9 ^d	54.6 ^f	-
BuS	6.0 ^c	37.4	-
Sulf.	4.4	35.6 ^g	35
<i>m</i> -NBA	N/A	50 ^h	-
PS	6.0	40.2	-

^a Abbreviations: 1,2-butylene carbonate (BC), 4-vinyl-1,3-dioxalan-2-one (4V), propylene carbonate (PC), ethylene carbonate (EC), 1,4-butanedisulfone (BuS), sulfolane (Sulf.), *m*-nitrobenzyl alcohol (*m*-NBA), and 1,3-propanedisulfone (PS). ^b Unless stated otherwise, all values were obtained from *CRC Handbook of Chemistry and Physics*, 95th Ed.; Lide, D.R., Ed.; CRC Press: Boca Raton, FL, 2014. ^c Park, M. H., *et al.*, *J. Power Sources* **2011**, *196*, 5109 (calculated values). ^d Chernyak, Y., *J. Chem. Eng. Data* **2006**, *51*, 416. ^e *Physical Chemistry of Surfaces*, 6th Ed.; Adamson, A. W.; Gast, A. P.; Wiley, 1997. ^f Naejus, R., Lemordant, D., Coudert, R., Willmann, P.: *J. Chem. Thermodynamics* **1997**, *29* 1503. ^g Kelayeh, S. A.; Jalili, A. H.; Ghotbi, C.; Hosseini-Jenab, M.; Taghikhani, V. *J. Chem. Eng. Data* **2011**, *56*, 4317 (30 °C). ^h Iavarone, A.T.; Jurchen, J.C.; Williams, E. R. *Int. J. Mass Spectrom.* **2002**, *219*, 63.

Table S3. Effects of acid concentration (prior to ESI) on the CSDs of protonated cytochrome *c* ions formed from acidified aqueous solutions containing 5 μ M cytochrome *c* and 5%(v/v) BC.

[HA] %(v/v)	Acetic Acid				Hydrochloric acid			
	$z_{\text{HOCS}}/z_{\text{MACS}}^a$	$\langle z \rangle^b$	W_z^c	Ad_{HA}^d	$z_{\text{HOCS}}/z_{\text{MACS}}^a$	$\langle z \rangle^b$	W_z^c	Ad_{HA}^d
0.5	26/23	22.6 \pm 0.2	1.6 \pm 0.2	7.3 \pm 1.0	16/13	13.6 \pm 0.1	2.7 \pm 0.1	71.2 \pm 3.2
1.0	26/22	21.8 \pm 0.1	1.8 \pm 0.3	8.3 \pm 1.8	16/13	13.6 \pm 0.1	2.8 \pm 0.2	80.8 \pm 2.5
1.5	24/21	21.2 \pm 0.1	2.0 \pm 0.3	10.3 \pm 2.1	16/12	12.5 \pm 0.1	3.4 \pm 0.3	81.3 \pm 6.4
2.0	24/21	20.8 \pm 0.1	2.1 \pm 0.2	13.6 \pm 2.2	16/12	12.3 \pm 0.1	3.5 \pm 0.3	83.4 \pm 9.1
2.5	23/20	20.5 \pm 0.2	2.3 \pm 0.4	15.6 \pm 2.2	15/12	11.8 \pm 0.1	4.2 \pm 0.7	87.6 \pm 10.3
3.0	23/19	18.6 \pm 0.1	2.2 \pm 0.3	17.7 \pm 2.0	n.o. ^e	n.o.	n.o.	n.o.
3.5	22/18	17.8 \pm 0.1	2.1 \pm 0.6	19.6 \pm 3.0				
4.0	22/18	17.4 \pm 0.3	2.4 \pm 0.5	21.3 \pm 2.1				
4.5	21/17	16.7 \pm 0.3	3.4 \pm 0.7	22.8 \pm 3.2				
5.0	21/17	16.6 \pm 0.1	3.5 \pm 0.8	38.9 \pm 5.1				

^a $z_{\text{HOCS}}/z_{\text{MACS}}$ are the highest observed charge state and the most abundant charge states. ^b Average charge state (standard deviation) of three replicate measurements. ^c Full-width-at-half maximum of Gaussian distributions that are fit to the observed charge state distributions (standard deviation values in parentheses). ^d extent of acid (HA) adduction (*i.e.*, [cyt *c*, $n\text{HA}, z\text{H}]^{z+}$). ^e Protein ions were not observed for HCl concentrations higher than 2.5%(v/v) under these conditions.

Table S4. ESI source capillary entrance to MS and tube lens potentials (V) that were used for each analyte (see Figure 3 and 4 of main text). For a given analyte, instrumental conditions were kept constant for different acids and superchargers used.

Protein/peptide	Capillary	Tube Lens
Angiotensin II	1.00	65.00
Ubiquitin	8.00	35.00
Cytochrome <i>c</i>	4.00	60.00
Myoglobin	4.00	70.00
Carbonic anhydrase II	6.00	80.00

Table S5. Henry's Law Constants (H^{cp} ; equilibrium partition coefficients between aqueous solutions and air; 25 °C and 1.0 bar), ^a boiling point values (b.p; 1.0 bar),^b vapour pressures (25 °C),^b and evaporation rates (e.r.; relative to butylacetate = 1)^b for acids of interest.

Acid	H^{cp} (mol m ⁻³ Pa ⁻¹)	b.p.(°C)	v.p. (mm Hg)	e.r.
HI	N/A	-35	5.9×10^3	-
HClO ₄	9.9×10^3	19 ^c	-	-
HCl	1.5×10^1	-85	3.5×10^4	-
H ₂ SO ₄	1.3×10^{13}	337	5.9×10^{-5}	-
HNO ₃	8.8×10^2	83	6.3×10^1	-
HIO ₃	-	-	-	-
H ₂ C ₂ O ₄ ^d	6.1×10^6	-	0.5×10^0	-
H ₃ PO ₄	-	407	2.9×10^{-2}	-
HCOOH	8.8×10^1	101	4.3×10^1	2.1
C ₆ H ₅ COOH	2.9×10^2	249	7.0×10^{-4}	-
CH ₃ COOH	4.0×10^1	118	1.6×10^1	1.0
C ₆ H ₅ OH	2.8×10^1	182	3.5×10^{-1}	-

^a R. Sander, *Atmos. Chem. Phys. Discuss.* **2014**, *14*, 29615. ^b Hazardous Substances Data Bank, National Library of Medicine (Bethesda, Maryland, United States). <http://toxnet.nlm.nih.gov> (accessed 15 December 2014). ^c Reduced pressure (11 mm Hg). ^d Melting point is 190 °C (decomposes).

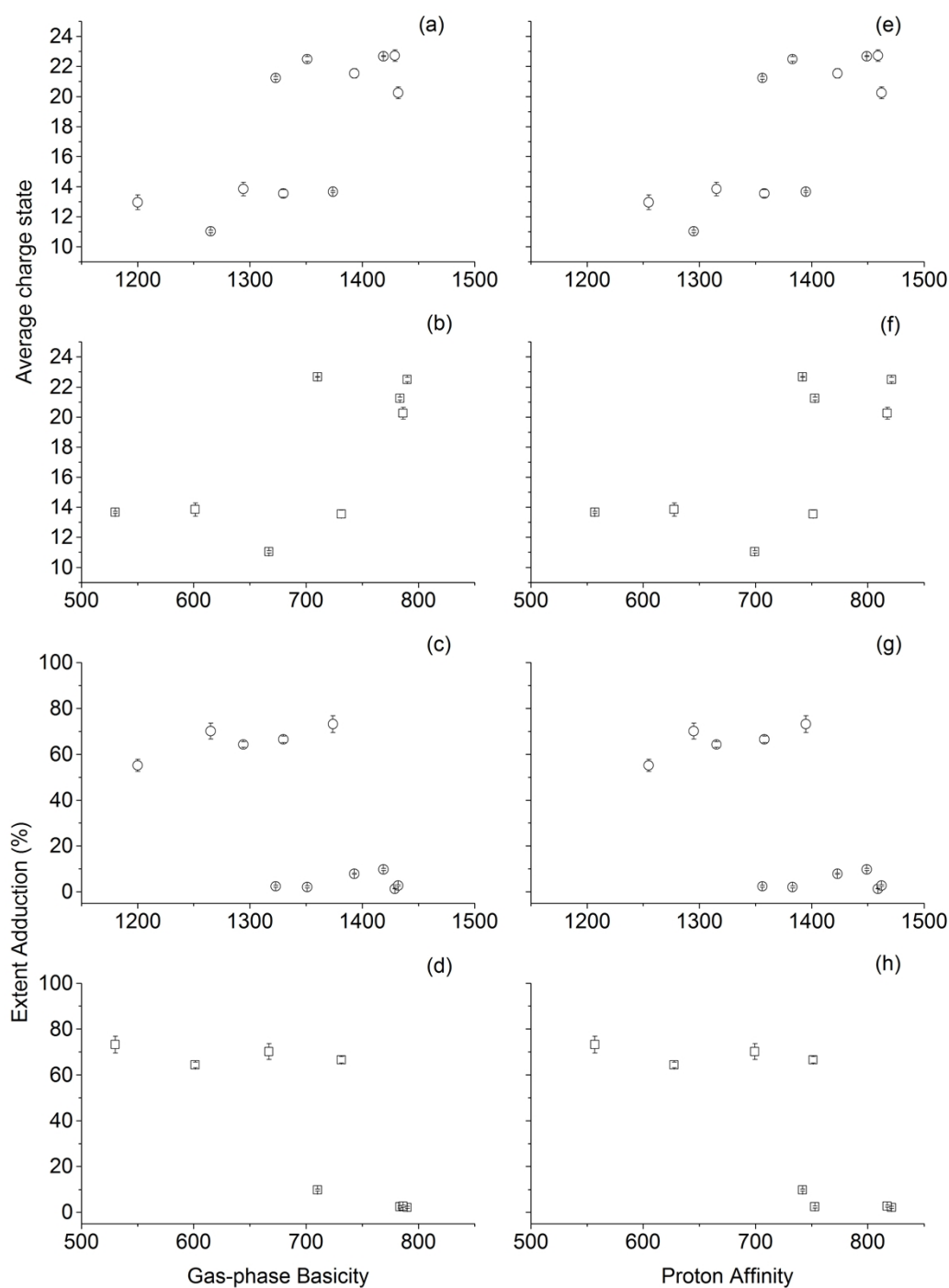


Figure S1. Effects of GB and PA of acids on the CSDs of protonated cyt *c* ions formed by ESI of solutions containing 5 μM cyt *c*, 0.5% acid (HI, HClO₄, HCl, H₂SO₄, HNO₃, HIO₃, H₂C₂O₄, H₃PO₄, HCOOH, C₆H₅COOH, CH₃COOH, C₆H₅OH), and 5% 4V (see Figure 3e). The average charge states of protonated cytochrome *c* ions vs. (a) GB of acid anion (A⁻), (b) GB of neutral acid (HA), (e) PA of A⁻, and (f) PA of HA. The extent of acid adduction for cytochrome *c* vs. (c) GB of acid anion (A⁻), (d) GB of neutral acid (HA), (g) PA of A⁻, and (h) PA of HA.

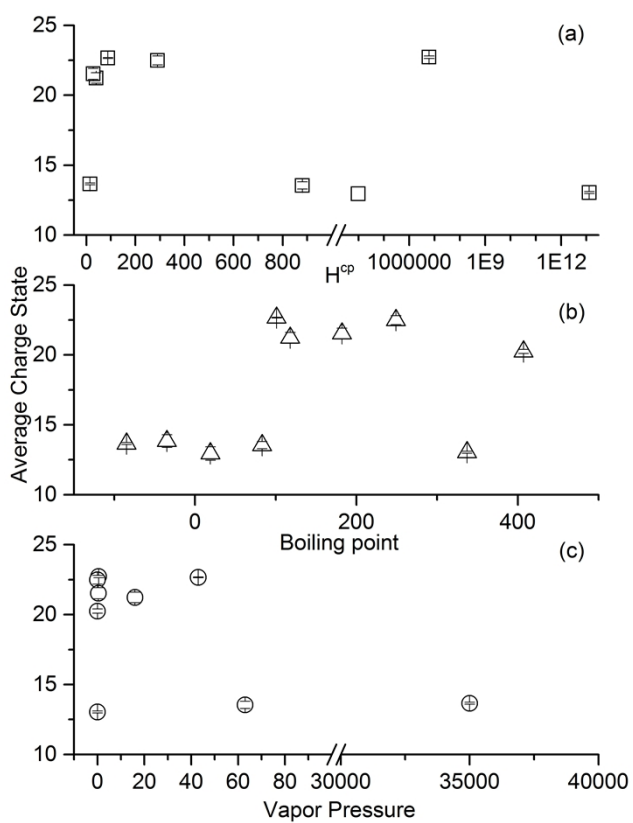


Figure S2. Average charge state for cytochrome *c* vs. the (a) Henry's Law Constants (H^{cp} ; equilibrium partition coefficients between aqueous solutions and air; 25 °C and 1.0 bar), (b) boiling points (1.0 bar) and (c) vapor pressures (25 °C) for acids of interest (same solutions as in Figure S1).

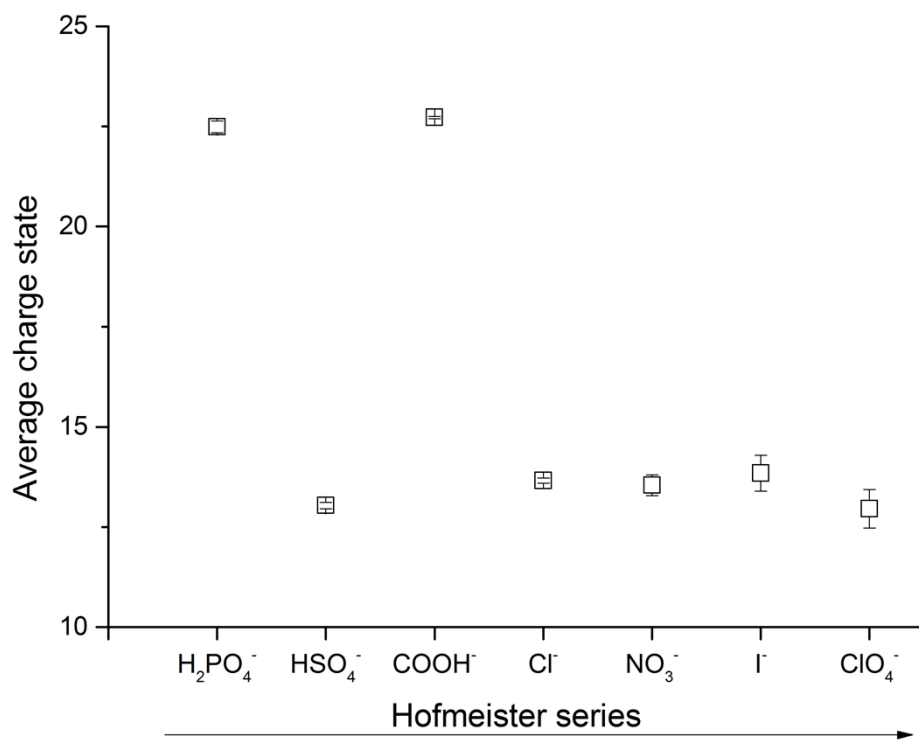


Figure S3. Average charge state of cytochrome *c* in order of the Hofmeister series (increasing protein destabilization from left to right) for acids of interest (same solutions as in Figure S1).

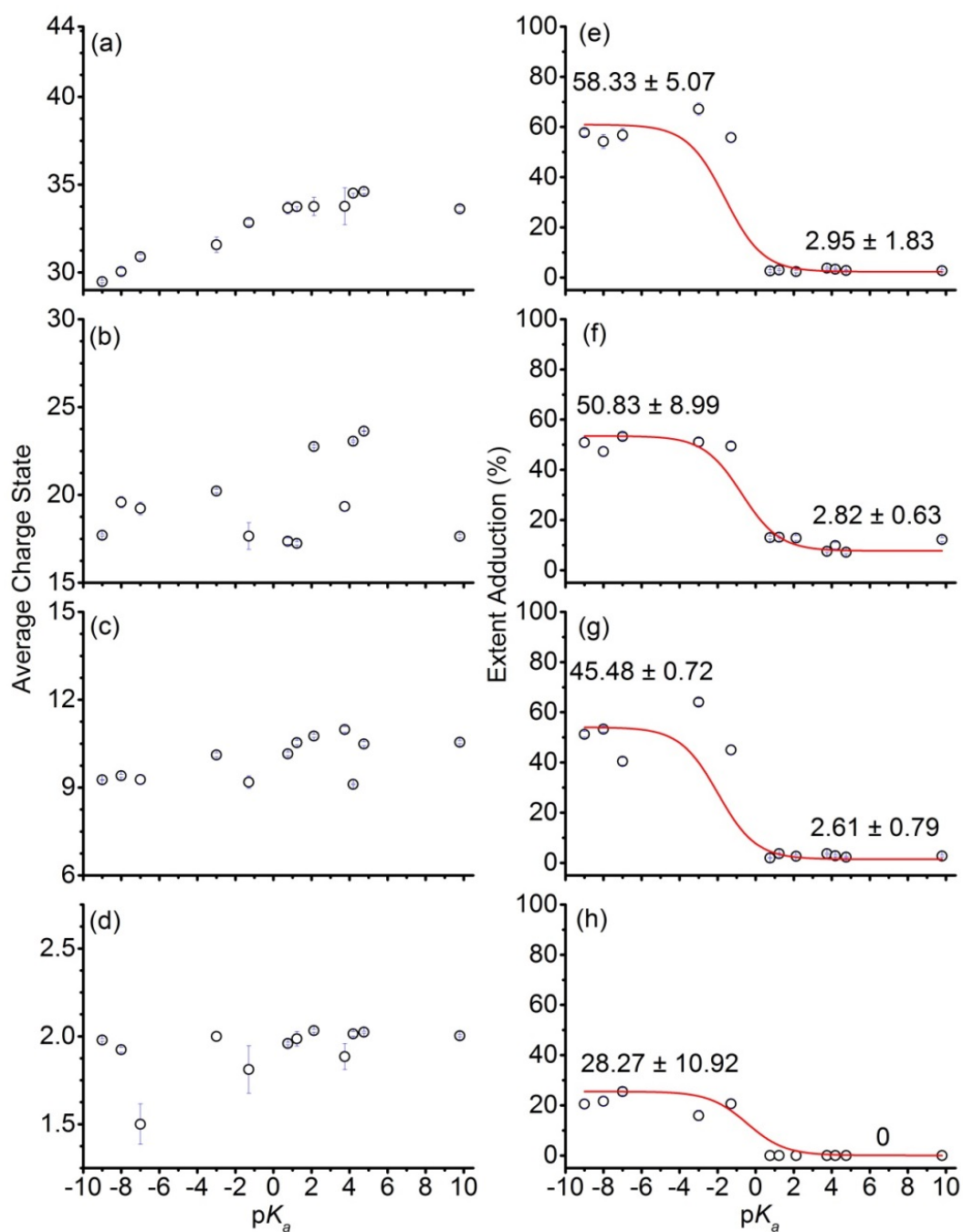


Figure S4. The average charge states (a-d) and extent of acid (HA) adduction (e-h) that were obtained from ESI mass spectra of aqueous solutions containing 0.5% acid (same acids as Fig. 3), and 5 μ M of either (a,e) CAII, (b,f) myoglobin, (c,g) ubiquitin, or (d,h) AII vs. the pK_a of the acid. The average ordinate values of 7 weak acids and 5 strong acids are given.

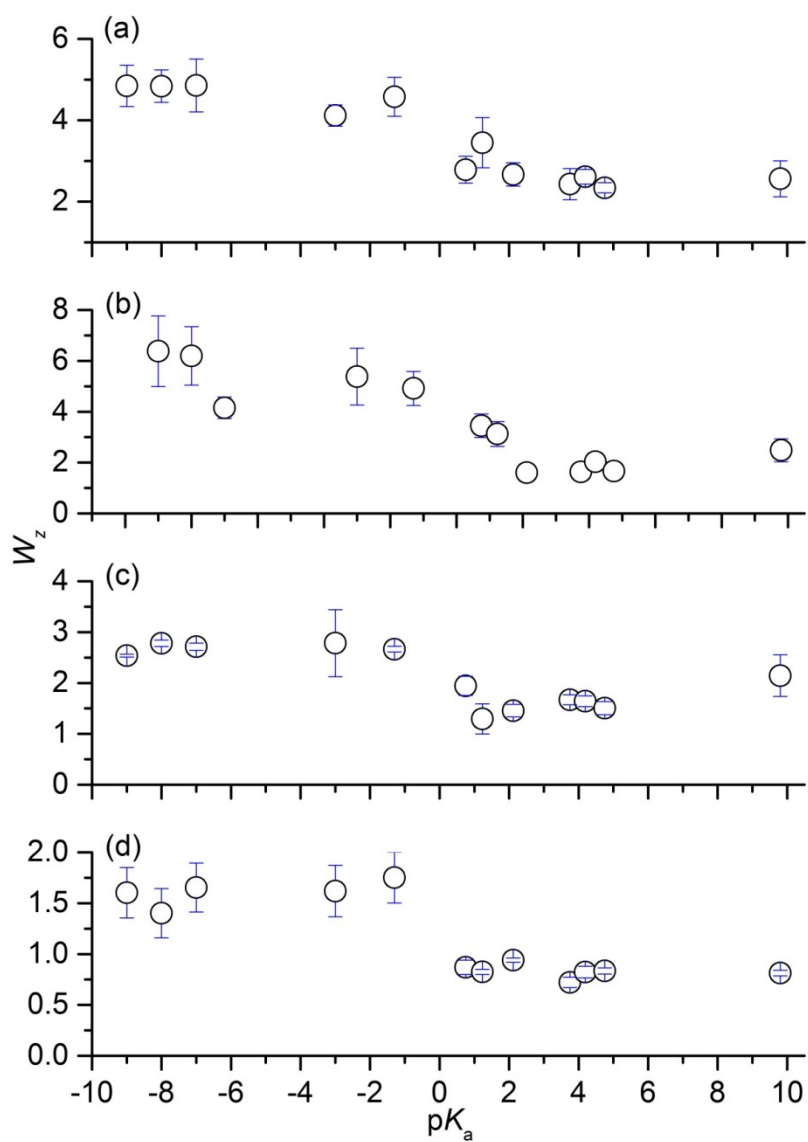


Figure S5. The full width at half maximum values (W_z) of protein ion charge state distributions that were obtained from ESI mass spectra of aqueous solutions containing 5% 4-vinyl-1,3-dioxalan-2-one, 0.5% acid (same acids as in Fig. 3), and 5 μ M (a) carbonic anhydrase II, (b) myoglobin, (c) cytochrome *c*, and (d) ubiquitin vs. the pK_a of the acid.

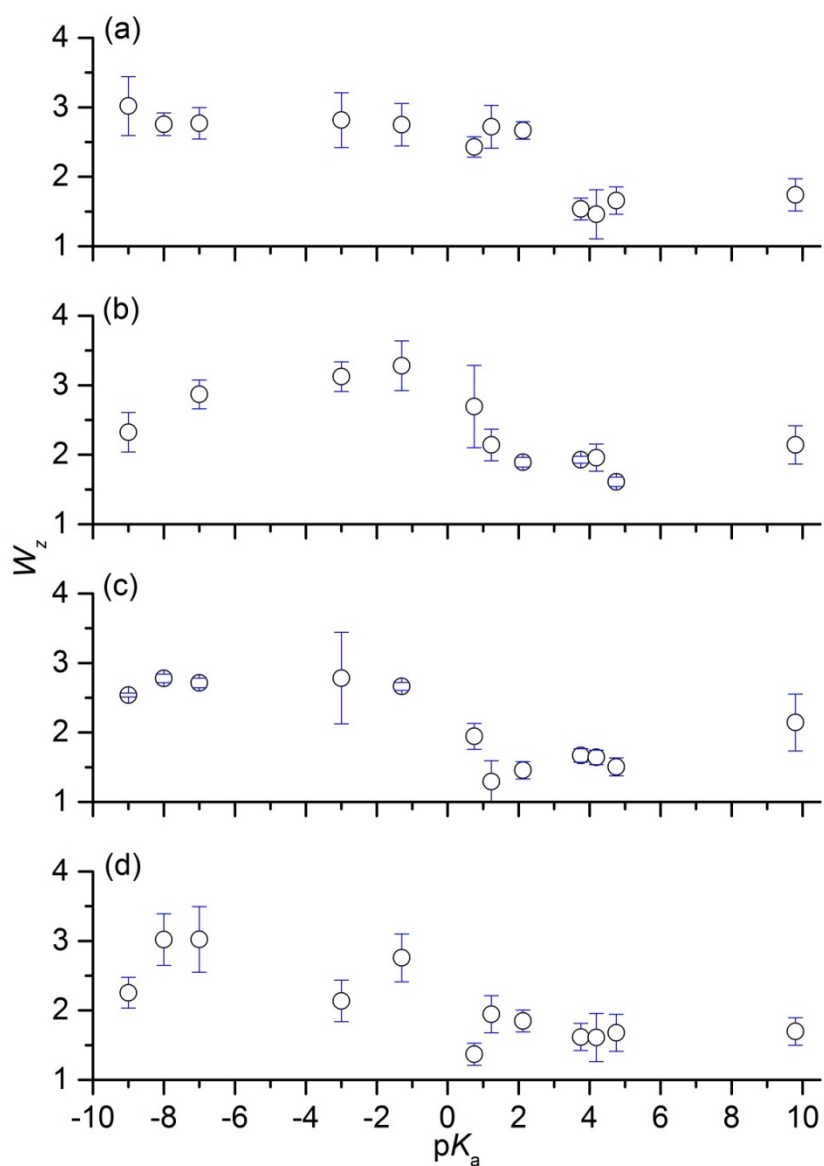


Figure S6. The full width at half maximum values (W_z) of protein ion charge state distributions that were obtained from ESI mass spectra of aqueous solutions containing 5 μ M cytochrome *c*, 0.5% acid (same acids as in Fig. 3), and 5% (a) 4-vinyl-1,3-dioxolan-2-one, (b) 1,4-butane sultone, (c) sulfolane, and (d) 1,3-propane sultone vs. the pK_a of the acid.

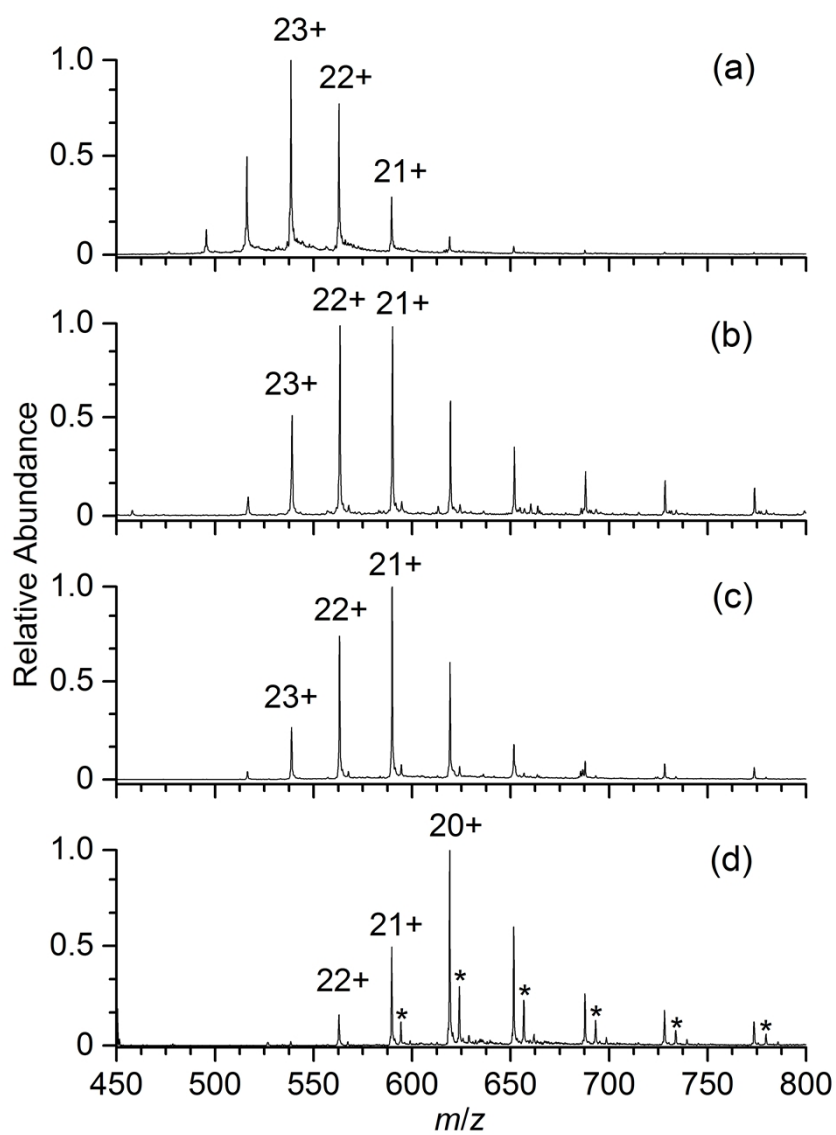


Figure S7. ESI mass spectra of solutions containing 5 μ M cytochrome *c*, 5% 4-vinyl-1,3-dioxalan-2-one, 0.5% acetic acid in (a) water, (b) methanol, (c) acetonitrile, and (d) isopropanol. An ion series corresponding to $[\text{cyt } c, z\text{H}, n(4\text{-vinyl-1,3-dioxalan-2-one})]^{z+}$ is denoted by “*”.

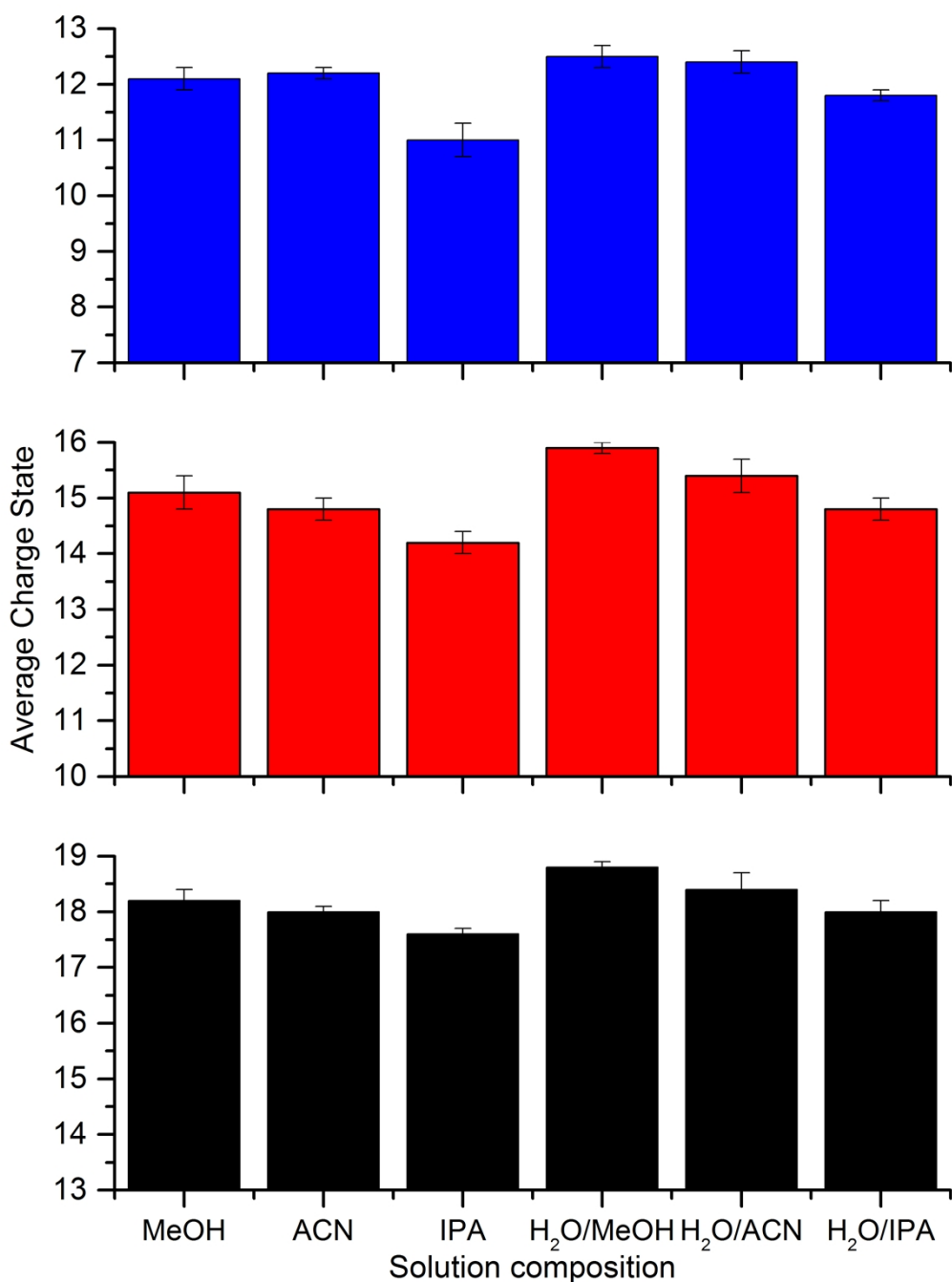


Figure S8. Average charge states of protonated (a) myoglobin, (b) cytochrome *c*, and, (c) ubiquitin ions that are formed by ESI of solutions containing 5 μ M protein, 0.5% acetic acid in methanol (MeOH), acetonitrile (ACN), isopropyl alcohol (IPA), 50/50 water/methanol, 50/50 water/acetonitrile, and 50/50 water/isopropyl alcohol.

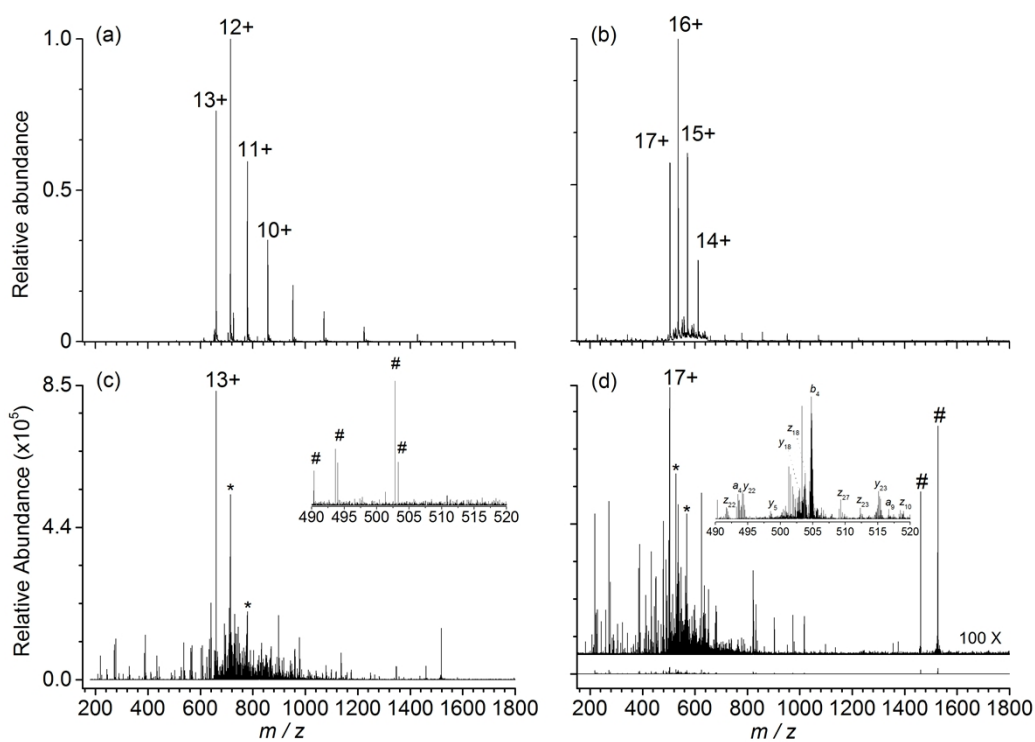


Figure S9. ESI mass spectra for aqueous solutions of 5 μM ubiquitin, 0.5% acetic acid, and (a) no supercharging additive, and (b) 5% 1,2-butylene carbonate. ECD mass spectra of the most abundant charge state that can be readily isolated from each solution: (c) [ubiquitin, 13H] $^{13+}$ and (d) [ubiquitin, 17H] $^{17+}$. The ECD mass spectrum for [ubiquitin, 17H] $^{17+}$ is vertically expanded by a factor of 100. Peaks corresponding to the reduced precursor ions (first and second reductions) and instrumental noise are denoted by “*” and “#,” respectively.

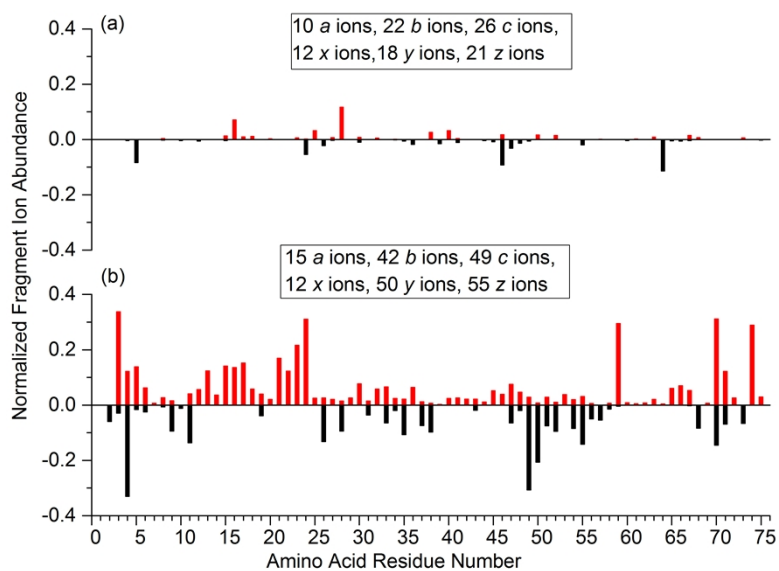


Figure S10. Relative ECD-MS fragment ion abundances at each inter-amino acid residue site for isolated (a) [ubiquitin, 13H]¹³⁺ and (b) [ubiquitin, 17H]¹⁷⁺. N-terminal and C-terminal fragments are given by respective positive (red) and negative values (black).

Methods

Analysis. The average charge states ($\langle z \rangle$) of protein ion charge state distributions were calculated by

$$\langle z \rangle = \frac{\sum(zI_z)}{\sum(I_z)} \quad (\text{S1})$$

where z is the charge state and I_z is the integrated abundance of each respective protein ion that is assigned in the mass spectrum. The widths of protein charge state distributions (CSDs) were approximated by fitting a Gaussian probability distribution to the CSDs of the protein ions.

Normalised protein ion abundances (*i.e.*, ion abundance values vs. protonation state) were fit to

$$I_z = A e^{-\frac{(z-\langle z \rangle)^2}{2\sigma^2}} \quad (\text{S2})$$

where σ is the standard deviation of the distribution and A is a normalization constant. By the definition, the full-width at half maximum of the CSD (W_z) is equal to 2.355σ . The extent of acid adduction to protein ions were calculated by

$$Add_{HA} = \frac{\sum I_a}{\sum I_a + \sum I_z} \quad (\text{S3})$$

where I_a and I_z are the respective ion abundances of [protein, nHA , zH] $^{z+}$ and [protein, zH] $^{z+}$ for all charge states. Mass spectra that were used to calculate $\langle z \rangle$, W_z and Add_{HA} were obtained on a LTQ-MS (see main text). High resolution FT-ICR mass spectra (7 LTQ-FT/ICR-MS) were obtained and compared to theoretical isotope distributions to support ion assignments (*e.g.*, Figure 1, main text).

Sequence ions were assigned by comparing measured m/z values and isotopic distributions of fragment ions to those for all possible sequence ions. Sequence coverage is defined as the number of unique inter-residue cleavage sites between adjacent amino acids that were identified in the tandem mass spectrum of interest out of the total number of inter-residue sites. The efficiency of electron capture (Eff_{ECD}) was calculated by

$$Eff_{ECD} = \frac{\sum I_F + I_R}{\sum I_F + I_R + I_P} \quad (\text{S4})$$

$$Eff_{Frag} = \frac{\sum I_F}{\sum I_F + I_R + I_P} \quad (\text{S5})$$

where $\sum I_F$ is the sum of the integrated abundances for each fragment ion, and I_R and I_P are the integrated abundances of the reduced and isolated precursor ions, respectively. The ECD fragmentation efficiency (Eff_{Frag}^*) was calculated by Eq. S5. The difference in Eff_{Frag}^* and Eff_{ECD} corresponds to the fraction of the reduced precursor ions that result in bond cleavage, separation of the fragments, and detection of the resulting product ions. Because the relative abundance of ions that are detected by FT/ICR-MS increase proportionally with charge state (see Ref. 2 in the main text), the ion abundances are normalized by the charge state of each ion for calculations using Eq. S4 and S5.

Circular dichroism measurements. Aqueous CD solutions contained 50 μ M of cyt *c*, 0.5% acid (HI, HClO₄, HCl, H₂SO₄, HNO₃, HIO₃, H₂C₂O₄, H₃PO₄, HCOOH, C₆H₅COOH, CH₃COOH, or C₆H₅OH), and either 5%(v/v) 4-vinyl-1,3-dioxolan-2-one or no 4-vinyl-1,3-dioxolan-2-one. To investigate the effects of 4-vinyl-1,3-dioxolan-2-one on protein structure, solutions containing 50 μ M of cyt *c*, 0.5% acetic acid and between 0 and 9% 4-vinyl-1,3-dioxolan-2-one were used. Circular dichroism (CD) experiments were performed using a Chirascan Plus spectrometer (Applied Photophysics) by use of instrument parameters that were recommended by the instrument manufacturer for analysis of cytochrome *c* (1 nm bandwidth; 0.5 nm increments; 0.1 mm pathlength, 3 s per data point, N₂ flow of 5 L/min). CD spectra were acquired for wavelengths from 185 to 240 nm. Control CD spectra of solutions that did not contain cyt *c* were subtracted from the CD spectra of solutions that contained cyt *c* (average of duplicates).¹ The CD trace was smoothed with a Savitzky-Golay filter (third order polynomial; 20 point smoothing window).¹ The CD spectrum that was obtained for cytochrome *c* in water (Figure 5) was in close agreement to the standard reference spectrum that was reported for this protein by the instrument manufacturer and that reported by Lees et al.² CD spectra were deconvoluted by use of CONTIN (Dichroweb; University of London),³⁻⁴ in which a linear superposition of the CD spectra of 16 standard proteins were fit to the CD spectra to obtain the relative fraction of unordered cyt *c*.

Solution-phase pH measurements. The pH of ESI solutions were measured using a pH meter (Cyberscan PCD 6500, Eutech Instruments, Singapore), which was calibrated using three standard solutions (pH buffer kit, model no. ECPHBUFKITC, Eutech Instruments, Singapore). For MilliQ water (18 M Ω), the pH value was measured to be 7.0 pH units (standard deviation < 0.1 pH units). Measurements were performed in triplicate (4 mL of solution per replicate). The standard deviations of the triplicate measurements were all < 0.1 pH units. The fraction of ionized acids (Figure 3a) prior to ESI were obtained from the pH measurements and the Henderson-Hasselbalch equation.

Surface tension measurements. The surface tensions of 4V, BC, PC and Sulf were measured by use of a dynamic surface tensiometer (DST9005, NIMA Technology, Coventry, UK) using the Du Noüy ring method (2 cm ring; 600 μ m outer diameter), in which the force required to remove a ring from a liquid is measured as a function of the distance between the ring and the liquid surface.⁵ The programmed ring immersion and withdrawal was set to immerse the ring 3 mm below the liquid level (immersion/withdrawal speed was 5 mm/min; liquid volume of 4 mL). Plots of force vs. immersion/withdrawal distance were collected in triplicate at ambient temperature (*ca.* 22 °C). By fitting the force-immersion curves, the surface tension values were obtained using the native tensiometer software. By use of this method, the surface tension of MilliQ water (18 M Ω) was measured to be 72.0 \pm 0.2 mN/m, which was near the literature value at 25 °C (71.9 mN/m).⁶ Based on comparison with literature data (Table S2) and considering that the standard deviation of triplicate measurements were < 1 mN/m, we approximate the uncertainty in the surface tension values that were obtained by use of experimental measurements to be \pm 2 mN/m.

Materials. Ubiquitin (bovine red blood cells; 8.6 kDa), carbonic anhydrase II (bovine erythrocytes; 29 kDa), and myoglobin (equine heart; 17 kDa) were obtained from Sigma-Aldrich. Cytochrome *c* (equine heart; 12 kDa) and angiotensin II (human; 1.0 kDa) were obtained from Alfa Aesar. 1,2 butylene carbonate was obtained from Tokyo chemical industries (TCI). 4-vinyl-1,3-dioxalan-2-one, propylene carbonate, 1,3-propane sultone, 1,4-butane sultone, sulfolane, and *m*-NBA were obtained from Sigma-Aldrich. These superchargers were used without any further

purification. Acetonitrile, isopropanol, methanol, HI, HClO₄, HCl, H₂SO₄, HNO₃, HIO₃, H₂C₂O₄ (anhydrous), H₃PO₄, HCOOH, C₆H₅COOH, CH₃COOH, and C₆H₅OH were obtained from Ajax Finechem.

Hofmeister effects

The extent of charging does not correlate with the Hofmeister series (Figure S3), which is the relative extent that anions destabilize protein structure:^{7, 8}



For example, by use of phosphoric acid (H₂PO₄⁻/H₃PO₄; high-protein stabilization end of Hofmeister series) the charging of cyt *c* is slightly lower ($\langle z \rangle = 20.6 \pm 0.2$) than by use of acetic acid (middle of Hofmeister series; $\langle z \rangle = 22.6 \pm 0.2$; Figure S3). In contrast, the extent of cyt *c* charging by use of sulphuric acid, which is between acetate and dihydrogenphosphate in the Hofmeister series, is significantly lower ($\langle z \rangle = 13.0 \pm 0.1$) than that for both acetic acid and phosphoric acid; *i.e.*, protein charging in ESI by use of different acids does not correlate with the Hofmeister series. Williams and co-workers determined that the extent of “electrothermal” supercharging of proteins from native solutions (increasing protein charging by increasing the electric field between the ESI capillary and the capillary entrance to the mass spectrometer) that contained ammonium salts of a range of Hofmeister anions strongly correlated with a reverse Hofmeister series.⁹ In our experiments, the proteins are largely denatured in these acidified solutions (see main text) and thus, protein structural effects are not expected to significantly affect the extent of analyte charging in ESI.

References

- (1) Greenfield, N. J., *Nat Protoc* **2006**, *1*, 2876.
- (2) Lees, J. G., *et al.*, *Bioinformatics* **2006**, *22*, 1955.
- (3) Whitmore, L. a. W., B.A., *Nucleic Acids Res.* **2004**, *32*, 5.
- (4) Whitmore, L. a. W., B.A., *Biopolymers* **2008**, *89*, 8.

- (5) (a) du Noüy, P. L., *J Gen. Physiol.* **1925**, *7*, 625; (b) Huh, C.; Mason, S. G., *Colloid Polym. Sci.* **1975**, *253*, 566.
- (6) Haynes, W. M., *CRC Handbook of Chemistry and Physics, 95th Edition*. Taylor & Francis: 2014.
- (7) Zhang, Y.; Cremer, P. S., *Curr. Opin. Chem. Biol.* **2006**, *10*, 658.
- (8) Hou, M.; Lu, R.; Yu, A., *RSC Advances* **2014**, *4*, 23078.
- (9) Cassou, C. A.; Williams, E. R., *Anal. Chem.* **2014**, *86*, 1640.